Journal of Pain Research

Dovepress
Taylor & Francis Group

Open Access Full Text Article

REVIEW

Structural and Functional Brain Alterations in Postherpetic Neuralgia: A Systematic Review and Voxel-Wise Coordinate-Based Meta-Analysis via the SDM-PSI Method

Yangching Na[1,2,*], Hongyu Mu[2,*], Jiarun Zhang[1,2], Qiuyi Chen[2], Luopeng Zhao[2], Zhongjian Tan[3], Lu Liu[2], Tianli Lv[2], Bin Li[2]

[1]Graduate School, Beijing University of Chinese Medicine, Beijing, 100029, People's Republic of China; [2]Department of Acupuncture and Moxibustion, Beijing Key Laboratory of Acupuncture Neuromodulation, Beijing Hospital of Traditional Chinese Medicine, Capital Medical University, Beijing, 100010, People's Republic of China; [3]Department of Radiology, Dong Zhimen Hospital, Beijing University of Chinese Medicine, Beijing, 100700, People's Republic of China

*These authors contributed equally to this work

Correspondence: Bin Li; Tianli Lv, Email libin@bjzhongyi.com; lvtianli@bjzhongyi.com

Background: Postherpetic neuralgia (PHN) is a chronic neuropathic pain condition persisting after herpes zoster, often accompanied by emotional and functional impairment. Neuroimaging suggests central nervous system involvement, but reported structural and functional findings remain inconsistent.

Methods: We conducted a systematic review and voxel-wise coordinate-based meta-analysis using Seed-based d Mapping with Permutation of Subject Images (SDM-PSI). PubMed, Embase, Web of Science, CNKI, and WanFang were searched up to December 31, 2025. Eligible studies used whole-brain resting-state fMRI indices (ALFF, fALFF, or ReHo) or structural MRI with voxel-based morphometry (VBM), reporting standard MNI or Talairach coordinates. Random-effects SDM-PSI analyses were performed for PHN versus healthy controls (HC), PHN versus herpes zoster patients (HZ), and PHN pre- versus post-treatment. Sensitivity, heterogeneity, publication bias, and meta-regression analyses were also conducted.

Results: Twenty-one studies (31 datasets) were included. Compared with HCs, PHN patients showed increased activity in the right cuneus, left putamen, and right anterior thalamic projections, and decreased activity in the right fusiform gyrus. Structural analyses revealed gray-matter reductions in the left Heschl's gyrus, right precentral gyrus, left postcentral gyrus, and left median cingulate/paracingulate cortex. Compared with HZ patients, PHN showed increased activity in bilateral cerebellar Crus II and decreased activity in the right superior parietal gyrus. Pre- versus post-treatment comparisons revealed limited alterations in the left median cingulate/paracingulate gyri and right lingual gyrus. Major clusters remained robust in sensitivity analyses, with low-to-moderate heterogeneity.

Conclusion: PHN is associated with convergent structural and functional alterations across cross-modal sensory, affective–cognitive, and cortico–basal ganglia networks. These network-level abnormalities may provide candidate neuroimaging biomarkers for characterizing PHN-related disease state and pain chronicization, as well as preliminary treatment-related neuroimaging features reflecting neuroplasticity. They may also guide future mechanism-based interventions, including network-level neuromodulation strategies. Further longitudinal and interventional studies are needed to validate their clinical utility.

Keywords: Postherpetic neuralgia, voxel-based morphometry, resting-state fMRI, ALFF, fALFF, ReHo, SDM-PSI, coordinate-based meta-analysis, chronic neuropathic pain

Introduction

Postherpetic neuralgia (PHN) is a debilitating form of chronic neuropathic pain that persists for at least one month following the resolution of herpes zoster (HZ) skin lesions. It primarily affects older adults and is marked by spontaneous pain, allodynia,

https://doi.org/10.2147/JPR.S600570
Received: 3 February 2026
Accepted: 9 May 2026
Published: 26 May 2026

and hyperalgesia localized to the affected dermatome.[1] PHN is frequently accompanied by psychological comorbidities such as anxiety and depression, leading to substantial impairment in quality of life.[2] Although both pharmacological and non-pharmacological treatments are available, their efficacy remains limited, and the central mechanisms underlying PHN remain incompletely understood, particularly the distributed brain network alterations supporting pain persistence.[3,4]

Neuroimaging studies have increasingly been used to explore pain-related brain alterations in PHN. Resting-state functional magnetic resonance imaging (rs-fMRI) studies have reported abnormal spontaneous brain activity, often assessed with indices such as amplitude of low-frequency fluctuations (ALFF), fractional ALFF (fALFF), and regional homogeneity (ReHo). Structural MRI (sMRI) studies have revealed gray matter changes in regions implicated in pain processing and modulation. However, the results across individual studies are inconsistent, with differences in sample size, imaging protocols, and analysis methods contributing to heterogeneity.

A growing body of research has identified structural and functional abnormalities in key regions of the so-called "pain matrix", including the thalamus, insula, amygdala, parahippocampal gyrus, precentral gyrus, dorsolateral prefrontal cortex (DLPFC), cingulate cortex, somatosensory cortices, precuneus, lentiform nucleus, and brainstem.[5,6] These regions are implicated in the sensory-discriminative, affective-emotional, and cognitive-modulatory dimensions of pain processing, suggesting that PHN involves widespread alterations in both pain perception and regulation. Nevertheless, despite these advances, the neuroimaging findings across PHN studies remain inconsistent, largely due to methodological heterogeneity. Differences in imaging modalities, scanning protocols, pre-processing pipelines, statistical approaches, sample sizes, and patient characteristics all contribute to divergent results.[7,8] Such inconsistencies hinder the establishment of a unified understanding of PHN-related neurobiological mechanisms, underscoring the need for meta-analytic techniques to synthesize available evidence and clarify the central features of PHN-related brain alterations.

To date, no coordinate-based meta-analysis has quantitatively synthesized brain imaging findings in PHN, as confirmed by our systematic search of PubMed, Embase, and Web of Science up to December 31, 2025. Existing studies have employed diverse comparison designs, including PHN versus healthy controls,[9–24] PHN versus HZ patients,[15,20,22,23,25,26] and longitudinal assessments of PHN patients pre- and post-treatment.[13,27–29] These methodological variations highlight the need for an integrated meta-analytic approach to identify robust and convergent patterns of PHN-related brain alterations.

To address this gap, we conducted a multimodal voxel-wise coordinate-based meta-analysis using Seed-based d Mapping with Permutation of Subject Images (SDM-PSI), an advanced approach that integrates reported peak coordinates and full statistical maps.[30,31] Compared with earlier techniques such as Activation Likelihood Estimation (ALE), SDM-PSI incorporates rigorous permutation testing, threshold-free cluster enhancement (TFCE), and a random-effects model to reduce false positives and account for between-study heterogeneity, thereby improving both sensitivity and specificity.

We first conducted unimodal meta-analyses of structural MRI studies using VBM to assess gray matter volume, and resting-state fMRI studies using ALFF, fALFF, and ReHo to examine spontaneous brain activity. Subgroup and heterogeneity analyses were subsequently applied to test the robustness of the primary results. Meta-regression analyses were also performed to explore the associations between neuroimaging findings and relevant clinical variables, such as mean age, pain duration, gender ratio, and pain intensity (VAS scores).

This multimodal meta-analysis aimed to identify robust structural and functional neuroimaging signatures of PHN, clarify its central mechanisms, and provide a quantitative foundation for future mechanistic and therapeutic research. The detailed methodology is described in the following sections.

Methods

Search Strategy

This review was conducted in accordance with PRISMA guidelines,[32] and the completed PRISMA checklist is provided in Supplementary Table 1. The review was prospectively registered in the PROSPERO database (Registration number: CRD420251030103). Five electronic databases were searched including PubMed, Web of Science, Excerpta Medica (Embase), Chinese National Knowledge Infrastructure (CNKI) and WanFang Data from their inception to December 31, 2025 (Figure 1). No restrictions were applied to the year of publication. The search terms included a combination of

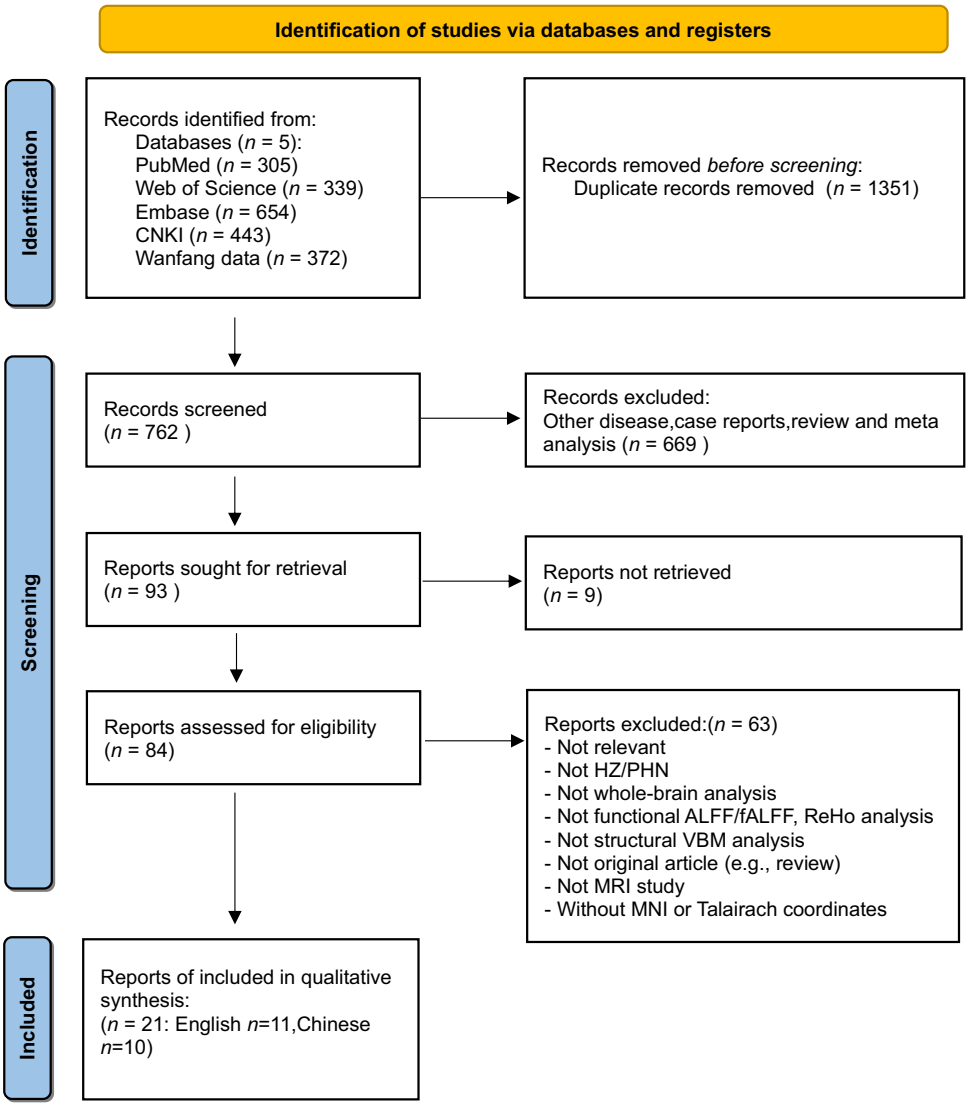

Figure 1 PRISMA 2020 flow diagram for new systematic reviews which included searches of databases and registers only.

neuroimaging modalities and PHN-related terms, such as: (Functional Magnetic Resonance Imaging OR Magnetic Resonance Imaging OR Voxel-Based Morphometry OR Surface-Based Morphometry OR Arterial Spin Labelling OR Resting-State fMRI OR Functional Connectivity OR Amplitude of Low-Frequency Fluctuation OR Fractional Amplitude of Low-Frequency Fluctuation OR Regional Homogeneity OR Diffusion Tensor Imaging OR Gray Matter Volume OR White Matter) AND ("Postherpetic Neuralgia" OR "Herpes Zoster Neuralgia" OR "Zoster-Associated Pain" OR "Herpes Zoster Pain" OR "Post-Shingles Pain"). This search strategy was modified to be suitable for Chinese electronic databases. Search strategies were adapted appropriately for Chinese databases (Supplementary Table 2). Additionally, the reference lists of included studies and relevant reviews were manually screened to identify potentially missed articles. After duplicate removal, two independent reviewers (NYC and MHY) screened the titles and abstracts for eligibility.

Eligibility and Exclusion Criteria

Inclusion Criteria

1. Adults (≥18 years old) diagnosed with PHN, defined by persistent neuropathic pain lasting more than 1 month after the resolution of shingles rash, in accordance with clinical diagnostic standards.

https://doi.org/10.2147/JPR.S600570

2. Comparative designs including PHN vs HCs, PHN vs HZ patients, or longitudinal comparisons pre- and post-treatment in PHN patients.
3. HC and HZ groups matched to PHN in age and sex.
4. Eligible studies included those using either resting-state fMRI (ALFF, fALFF, or ReHo) or structural MRI (VBM) conducted at the whole-brain level. For ALFF and fALFF analyses, the conventional frequency range of 0.01–0.08 Hz was required.
5. Studies must report 3D peak coordinates in standard stereotactic space (either Montreal Neurological Institute [MNI] or Talairach space).
6. Studies should include at least 10 participants per group (eg, PHN and HC). However, studies with smaller sample sizes may be included if they contribute unique longitudinal or treatment-related imaging data and meet other methodological criteria.

Exclusion Criteria

1. Incomplete or unavailable neuroimaging data, including studies that did not report standard three-dimensional coordinates (MNI or Talairach) from resting-state fMRI (eg, ALFF, fALFF, ReHo) or structural MRI (eg, VBM), even after contacting the corresponding authors.
2. Lack of whole-brain analysis, including those limited to region-of-interest (ROI) analyses without voxel-wise comparisons across the entire brain.
3. Non-original research, such as reviews, meta-analyses, case reports, conference abstracts, editorials, or letters to the editor.
4. Studies not published in English or Chinese, unpublished manuscripts, conference abstracts, and non-academic sources were excluded; academic theses or dissertations were eligible if they met the same coordinate-reporting and methodological quality criteria as published articles.

Corresponding authors of the original studies were contacted by phone or Email when data were unavailable or unclear. To avoid duplicate inclusion of overlapping samples, only the article with the largest sample size and the most comprehensive information was included when two or more studies used the same data source. For longitudinal or intervention studies, baseline data and eligible pre- and post-treatment contrasts were analyzed separately according to the corresponding comparison.

Data Extraction

Two independent reviewers (NYC, MHY) screened articles by title and abstract for relevance. These studies were then screened for eligibility through full-text evaluation. For each included article, two independent reviewers extracted data. Any disagreements were resolved through collaboration with a third reviewer (LTL). Detailed instructions on the type of information to extract were also discussed among the team members. The following information was extracted from each manuscript: (a) authors and year of publication; (b) participant characteristics (sample size, mean age, sex ratio, years of education); (c) study design; (d) pain duration; (e) MRI acquisition parameters (MRI scanner magnetic field strength, timing to scan, software, slice thickness, FWHM, thresholds for significance corrected for multiple comparisons or uncorrected, etc); (f) rs-fMRI methodology; (g) clinical assessment scales, primarily the Visual Analog Scale (VAS), as this was the only consistently reported clinical pain measure across studies. Coordinates from each study were independently extracted following the SDM-PSI requirements. When both corrected and uncorrected results were reported in an rs-fMRI or sMRI study, corrected results were preferentially extracted to reduce the risk of false-positive findings. As detailed in Supplementary Table 3, the extracted data and eligibility of each included article were then validated by an independent reviewer (NYC).

Neuroimaging Data Synthesis and Coding

All eligible studies were reviewed to extract the peak coordinates of brain regions showing significant group differences. For each study, the following information was collected: (1) sample size of each group; (2) diagnostic criteria; (3)

statistical values (eg, *t* or *z* scores) and corresponding *p*-values; (4) stereotactic coordinates (MNI or Talairach space); and (5) direction of the effect (increased or decreased activation/volume), as detailed in Supplementary Table 4.

When studies reported coordinates in Talairach space, these were converted to MNI space using the Lancaster transform (icbm2tal). If multiple contrasts were reported within a study (eg, different subgroups or time points), only the most relevant contrast for the current analysis was included to avoid double-counting of samples. For studies reporting only figures, coordinates were extracted using MRIcron or directly obtained from the authors if necessary. If no *t*-value was provided, we used the SDM website (https://www.sdmproject.com/) to convert the *p*-value or *z*-value into *t*-value.

Two independent reviewers (NYC, MHY) extracted the neuroimaging data, and any discrepancies were resolved through discussion or consultation with a third reviewer (LTL). The extracted coordinates and statistical information were formatted according to the SDM-PSI requirements for subsequent voxel-wise meta-analysis.

Quality Assessment

A customized quality checklist (20-point scale), adapted from previous neuroimaging meta-analyses, was used, and studies with a total score below 16 points were excluded.[33,34] The total score of the form was 20, with two parts of sample information (10 points) and imaging methods (10 points). A detailed list of quality assessments is provided in Supplementary Table 5. It evaluated diagnostic standardization, demographic and clinical reporting, sample size, scanning parameters, preprocessing procedures, analysis transparency, and discussion of study limitations. Two authors (NYC, MHY) independently assessed each study, and discrepancies were resolved via consensus within the team.

Voxel-Wise Meta-Analysis of Functional Differences

Voxel-wise meta-analyses of functional imaging data (ALFF, fALFF, and ReHo) were performed using the SDM-PSI (version 6.23beta, https://www.sdmproject.com/), following standardized procedures. SDM-PSI uses peak coordinates and corresponding *t*-values from each study to generate multiple imputed effect-size maps (Hedges' g) for increased and decreased activity, which are then combined using a random-effects model accounting for sample size, intra-study variability, and inter-study heterogeneity.[35] Rubin's rules were applied to pool multiple imputations,[31] and significance was tested using a permutation-based estimation of the family-wise error rate (FWER). The MetaNSUE algorithm was applied to estimate likely effect sizes while modelling uncertainty and realistic noise.[36] SDM maps were visualized using MRIcron software (https://www.mricro.com/mricron/).

Whole-brain meta-analyses were conducted for the following contrasts: PHN vs HC, PHN vs HZ, and PHN pre- and post-treatment. For the primary analysis, we applied a voxel-wise uncorrected threshold of $P < 0.005$, *p*eak SDM-$Z > 1$, and a minimum cluster extent of ≥10 voxels. This thresholding approach was selected with reference to previous SDM-based neuroimaging meta-analyses, including SDM-PSI studies, that used similar criteria in chronic pain and other neuropsychiatric conditions.[37–39] In addition, because a relatively small cluster extent may increase sensitivity but may also raise the possibility of false-positive findings, TFCE-based FWE correction ($P_{TFCE} < 0.05$, 5000 permutations) was applied as a complementary, more stringent analysis to test the stability of significant clusters.[40]

Voxel-Wise Meta-Analysis of Structural Differences

Voxel-wise meta-analyses of structural brain alterations based on VBM data were also conducted using the same SDM-PSI pipeline and thresholding strategy for the PHN vs HC, PHN vs HZ, and PHN pre- and post-treatment comparisons when eligible VBM datasets were available.

Robustness, Heterogeneity, and Publication Bias Analysis

To evaluate the robustness and reproducibility of the main meta-analytic findings, we performed a whole-brain voxel-based jack-knife sensitivity analysis by iteratively re-running the analysis while excluding one dataset at a time. This procedure was repeated *K* times, where *K* represents the total number of included datasets. If the major brain regions identified in the original analysis remained significant across most or all iterations, the findings were considered robust and highly replicable.

Between-study heterogeneity was assessed using the I^2 statistic.[41] A value of $I^2 \leq 50\%$ was interpreted as indicating low-to-moderate heterogeneity, suggesting that the proportion of variance attributable to between-study differences was within an acceptable range. Heterogeneity was assessed for significant clusters identified in the main meta-analytic analyses using the SDM-PSI random-effects framework. The relatively small cluster extent threshold (≥10 voxels) was adopted to improve sensitivity in detecting consistent but spatially limited effects. However, we acknowledge that this threshold may increase the risk of false-positive findings. Therefore, TFCE-based family-wise error correction was additionally applied as a more stringent validation to enhance the robustness of the findings.

Potential publication bias for significant clusters was evaluated by visually inspecting funnel plots and conducting Egger's test on peak coordinates.[42] A p-value < 0.05 in Egger's test, along with funnel plot asymmetry, was considered indicative of potential publication bias.[43]

Meta-Regression Analyses

Voxel-wise meta-regression analyses were performed using SDM-PSI to assess whether clinical and demographic variables, including mean age, sex ratio, pain duration, and VAS scores, contributed to the heterogeneity of the main meta-analytic results.

Statistical significance was assessed using TFCE-based family-wise error correction at $P_{TFCE} < 0.05$. Peak SDM-$Z >$ 1 was used for cluster reporting. Meta-regression analyses were conducted at the whole-brain level, and only moderator-related clusters that overlapped with significant regions identified in the main meta-analysis were interpreted, following recommended SDM-PSI procedures and prior meta-analytic studies.

Results

Included Studies and Sample Characteristics

A total of 21 studies comprising 31 datasets met the inclusion and exclusion criteria, including 11 published in English and 10 in Chinese. Among them, 12 rs-fMRI datasets investigating PHN patients versus HCs reported results using ALFF, fALFF, or ReHo indices, and 6 sMRI datasets employed VBM for the same comparison. For comparisons between PHN and HZ patients, 4 rs-fMRI and 3 VBM datasets were included. Additionally, 6 rs-fMRI datasets explored functional brain changes in PHN pre- and post-treatment. The demographic and clinical characteristics of all included studies are summarized in Table 1. All included studies achieved a quality score ≥ 17 on the 20-point checklist (Supplementary Table 5).

Functional and Structural Abnormalities Among Included Studies

A systematic synthesis of the included studies revealed convergent functional and structural abnormalities across the PHN vs HC, PHN vs HZ, and PHN pre- and post-treatment comparisons (Table 2). Most clusters survived the primary threshold (voxel-wise $P < 0.005$), whereas only a subset remained significant under TFCE-based FWE correction, consistent with the more conservative nature of TFCE.

Functional Alterations

Across the included datasets, PHN patients exhibited increased functional activity in the right cuneus cortex, left lenticular nucleus/putamen, and right anterior thalamic projections, while decreased activity was observed in the right fusiform gyrus relative to HCs (Figure 2a). When compared with HZ patients, PHN patients showed enhanced activation in the bilateral cerebellar Crus II, particularly in the left, and a reduction in the right superior parietal gyrus (Figure 3). In the longitudinal comparison between PHN pre- and post-treatment stages, only limited changes were detected, including increased activation in the left median cingulate/paracingulate gyri and decreased activation in the right lingual gyrus, suggesting subtle or heterogeneous treatment-related effects (Figure 4). TFCE-corrected glass-brain visualizations of the PHN vs HC, PHN vs HZ, and PHN pre- and post-treatment comparisons are provided in Supplementary Figures 1–4 to further illustrate the spatial distribution and direction of the more conservative meta-analytic findings.

Table 1 Demographic and Clinical Characteristics of Studies Included in the Functional Rs-fMRI and Structural VBM Meta-Analyses

Study	Year	PHN (Female), n	Mean Age ±SD, Year	Education Years	Pain Duration	Healthy (Female), n	Mean Age ±SD, Year	Education Years	Time (s)	Software	Slice Thickness (mm)	FWHM (mm)	Methodology	Threshold	*P*-value
PHN vs HC															
Functional															
ALFF/fALFF/ReHo															
Cao[9]	2019	23 (12)	71.26±8.43	8.39±3.62	3.83±7.26	23 (15)	69.78±9.05	9.78±3.45	420s	SPM8	3.5	4	ALFF	GRF corrected	*P*<0.01
Zhang[10]	2016	17 (8)	64.82±7.03	5.53±4.17	5.12±6.17	17 (10)	60.88±6.47	5.94±3.53	824s	DPARSF	4	8	fALFF, ReHo	AlphaSim corrected	*P*<0.05
Yi[11]	2017	15 (5)	61.53±13.25	9.12±3.0	6.60±NA	15 (5)	55.73±8.31	11.48±2.30	486s	DPARSF, SPM12	4	6	fALFF, ReHo	AlphaSim corrected	*P*<0.001
Liao et al[12]	2015	8 (4)	60.00 ±7.01	NA	10.75±5.52	8 (4)	61.15±6.54	NA	480s	SPM8	3.5	6	ALFF	AlphaSim corrected	*P*voxel<0.001, *P*cluster<0.05
Jiang[13]	2017	12 (5)	60.92±9.29	8.87±3.45	NA	12 (5)	61.75±8.82	9.26±5.53	480s	DPARSF, SPM8	4	4	ALFF, fALFF	AlphaSim corrected	*P*voxel<0.001, *P*cluster<0.05
Bai et al[14]	2022	34 (NA)	65.61±5.49	NA	NA	40 (NA)	64.45±3.48	NA	480s	SPM8	4	NA	ALFF	AlphaSim corrected	*P*voxel<0.001, *P*cluster<0.05
Cao[15]	2017	18 (9)	64.30±6.40	NA	13.60±19.60	20 (12)	60.30±5.80	NA	420s	DPARSF, REST	5	4	fALFF, ReHo	AlphaSim corrected	*P*cluster<0.05
Huang et al[16]	2020	24 (9)	67.00±14.10	NA	7.57 ± 2.40	20 (13)	63.10±12.20	NA	438s	DPARSF	3.6	6	ALFF	FDR corrected	*P*<0.05
Cao et al[17]	2017	19 (8)	64.40±2.10	NA	5.40±1.30	19 (11)	61.40±1.10	NA	420s	DPARSF	4	4	fALFF, ReHo	AlphaSim corrected	*P*voxel<0.05
Gu et al[18]	2019	18 (7)	59.67±8.41	NA	3.89±0.87	18 (7)	59.27±7.74	NA	480s	DPABI	4	4	ALFF	GRF corrected	*P*voxel<0.025, *P*cluster<0.05
Hui et al[19]	2020	12 (5)	60.92±9.29	8.87±3.45	NA	12 (5)	61.75± 8.82	9.26 ± 5.53	480s	DPABI, SPM8	4	6	ALFF, fALFF	AlphaSim corrected	*P*<0.05
Cao et al[20]	2017	23 (13)	65.90±2.30	NA	12.20±3.70	55 (24)	63.10±0.79	NA	420s	DPARSF	4	4	fALFF, ReHo	AlphaSim corrected	*P*voxel<0.05
Structural															
VBM															
Zhang[10]	2016	17 (8)	64.82±7.03	5.53±4.17	5.12±6.17	17 (10)	60.88±6.47	5.94±3.53	824s	SPM8	1	8	VBM	uncorrected	*P*<0.001
Jiang[13]	2017	12 (5)	60.92±9.29	8.87±3.45	NA	12 (5)	61.75±8.82	9.26±5.53	312s	SPM8	1	4	VBM	AlphaSim corrected	*P*voxel<0.001, *P*cluster<0.05
Wang et al[21]	2017	17 (6)	62.53±12.79	6.53± 1.81	4.15± 2.64	17 (8)	54.65±11.96	6.82± 1.42	696s	DPARSF	1	8	VBM	FDR corrected	*P*<0.05
Yu et al[22]	2021	28 (11)	63.07±7.90	NA	2.50±1.35	21 (9)	58.48±10.34	NA	546s	SPM8	1	8	VBM	AlphaSim corrected	*P*voxel<0.01, *P*cluster<0.05

(*Continued*)

https://doi.org/10.2147/JPR.S600570

https://doi.org/10.2147/JPR.S600570

Table 1 (Continued).

Liu et al[23]	2019	22 (13)	65.50±11.25	NA	2.00±2.25	28 (19)	54.00±9.75	NA	480s	DPARSF	1	8	VBM	GRF corrected	*P*voxel<0.01, *P*cluster<0.05
Li et al[24]	2022	25 (12)	63.0 ± 7.51	4.88 ± 2.18	5.12 ± 6.17	25 (15)	61.68± 8.09	5.72± 2.01	NA	SPM8	NA	NA	VBM	uncorrected	*P*<0.001
Study	**Year**	**PHN (Female), n**	**Mean Age ±SD, Year**	**Education Year**	**Pain Duration**	**HZ (Female), n**	**Mean Age ±SD, Year**	**Pain Duration**	**Time**	**Software**	**Slice Thickness (mm)**	**FWHM (mm)**	**Methodology**	**Threshold**	***P*-value**
PHN vs HZ															
Functional															
ALFF/fALFF/ReHo															
Cao[15]	2017	18 (9)	64.30±6.40	NA	13.60±19.60	32 (13)	60.80±6.00	0.90±0.60	420s	DPARSF, REST	5	4	fALFF, ReHo	AlphaSim corrected	*P*cluster<0.05
Liang[25]	2013	6 (3)	58.33±4.03	NA	4.00±1.67	6 (4)	59.17±3.12	0.38±0.04	420s	SPM8, REST	4	4	ALFF, fALFF	uncorrected	*P*<0.05
Cao et al[20]	2017	23 (13)	65.90±2.30	NA	12.20±3.70	50 (21)	60.50±1.80	0.98±0.10	420s	DPARSF, SPM8, REST	4	4	fALFF, ReHo	AlphaSim corrected	*P*voxel<0.05
Liang et al[26]	2014	6 (3)	58.33±4.03	NA	4.00±1.67	6 (4)	59.17±3.12	0.38±0.04	420s	SPM8, REST	4	4	ReHo	uncorrected	*P*<0.05
Structural															
VBM															
Cao[15]	2017	18 (9)	64.30±6.40	NA	13.6±19.6	32 (13)	60.80±6.00	0.90±0.60	628s	DPARSF, SPM8	1	8	VBM	AlphaSim corrected	*P*cluster<0.05
Yu et al[22]	2021	28 (11)	63.07±7.90	NA	2.50±1.35	25 (11)	59.00±9.84	0.44±0.25	546s	SPM8	1	8	VBM	AlphaSim corrected	*P*voxel<0.01, *P*cluster<0.05
Liu et al[23]	2019	22 (13)	65.50±11.25	NA	2.00±2.25	33 (20)	57.00±12.50	0.30±0.38	480s	DPARSF	1	8	VBM	GRF corrected	*P*voxel<0.01, *P*cluster<0.05
Study	**Year**	**PHN (female), n**	**Mean Age ±SD, year**	**Education years**	**Pain Duration**	**Treatment Duration**	**Treatment**	**Clinical Assessment Scales**	**Time**	**Software**	**Slice Thickness (mm)**	**FWHM (mm)**	**Methodology**	**Threshold**	***P*-value**
PHN Pre- and Post-Treatment															
Functional															
ALFF/fALFF/ReHo															
Jiang[13]	2017	12 (5)	60.92±9.29	8.87±3.45	NA	NA	NA	NA	480s	DPARSF, SPM 8	4	4	ALFF, fALFF	AlphaSim corrected	*P*voxel<0.001, *P*cluster<0.05
Chun et al[27]	2023	10 (5)	69.50±13.80	NA	3.25±2.35	0.5	stSCS	NA	412s	DPARSF, SPM 8	2.2	6	ALFF	GRF corrected	*P*voxel<0.001, *P*cluster<0.05
Zhang et al[28]	2020	15 (8)	64.13±7.33	NA	3.57±2.27	6	NA	VAS Baseline, VAS After Treatment	420s	DPARSF, SPM 8	4	4	fALFF, ReHo	AlphaSim corrected	*P*voxel<0.05
Fan et al[29]	2022	10 (5)	69.50±13.80	NA	3.25±2.35	0.5	stSCS	NA	420s	DPARSF, SPM 8	2.2	4	ReHo	GRF corrected	*P*voxel<0.005, *P*cluster<0.05

Notes: All included studies adopted the Montreal Neurological Institute (MNI) space for coordinate reporting, recruited right-handed patients, and employed 3.0 Tesla MRI scanners. Details of clinical assessment scales used in each study are summarized in Supplementary Table 3.

Abbreviations: ALFF, amplitude of low-frequency fluctuations; AlphaSim corrected, Monte Carlo simulation-based multiple comparison correction method; DPARSF, Data Processing Assistant for Resting-State fMRI; DPABI, Data Processing and Analysis for Brain Imaging; fALFF, Fractional Amplitude of Low-Frequency Fluctuations; FDR corrected, False Discovery Rate corrected; FWHM, full width at half maximum; GRF corrected, Gaussian Random Field corrected; ReHo, regional homogeneity; REST, Resting-State fMRI Data Analysis Toolkit; VBM, Voxel-Based Morphometry; SPM, Statistical Parametric Mapping.

Table 2 Significant Brain Regions Identified in the Meta-Analysis for Functional and Structural Alterations Across PHN Vs HC, PHN Vs HZ, and PHN Pre- and Post-Treatment Comparisons

Group	Change Type	Signal Enhancement	Threshold	Brain Region	MNI Coordinate	*P*-value	Voxels	SDM-*Z* value	$I^2_{(\%)}$	Jack-Knife Analysis
PHN vs HC	Functional changes	Increased	P_{TFCE}<0.05	Right cuneus cortex	8, −70, 24	0.007000029	220	4.412	2.702088	14/17
			$P_{uncorrected}$<0.005	Left lenticular nucleus, putamen	−30, −6, 0	0.000081658	286	3.77	2.166723	15/17
				Right anterior thalamic projections	14, −8, 12	0.001141012	29	3.051	38.669537	12/17
		Decreased	$P_{uncorrected}$<0.005	Right fusiform gyrus, BA 20	44, −36, −28	0.001525819	36	−2.962	18.143925	12/17
	Structural changes	Decreased	P_{TFCE}<0.05	Left Heschl's gyrus	−42, −16, 8	0.000999987	957	−4.511	2.795088	3/6
			$P_{uncorrected}$<0.005	Right precentral gyrus, BA 4	54, −6, 38	0.000620782	362	−3.229	15.924041	3/6
				Left median cingulate / paracingulate gyri	−2, −38, 44	0.001739502	228	−2.922	17.656252	2/6
				Left postcentral gyrus, BA 2	−42, −32, 44	0.001260817	20	−3.021	12.015899	3/6
PHN vs HZ	Functional changes	Increased	P_{TFCE}<0.05	Left cerebellum, crus II	−34, −76, −42	0.000999987	400	5.074	5.815318	6/6
			$P_{uncorrected}$<0.005	Right cerebellum, crus II	42, −72, −42	0.000319362	810	3.415	4.158621	4/6
		Decreased	P_{TFCE}<0.05	Right superior parietal gyrus, BA 7	28, −64, 50	0.000999987	370	−5.879	0.664024	6/6
PHN pre- and post-treatment	Functional changes	Increased	P_{TFCE}<0.05	Left median cingulate / paracingulate gyri	−12, −50, 32	0.019999981	97	2.724	14.841345	1/4
		Decreased	P_{TFCE}<0.05	Right lingual gyrus, BA 17	6, −80, −6	0.013000011	27	−4.123	0.996007	1/4

https://doi.org/10.2147/JPR.S600570

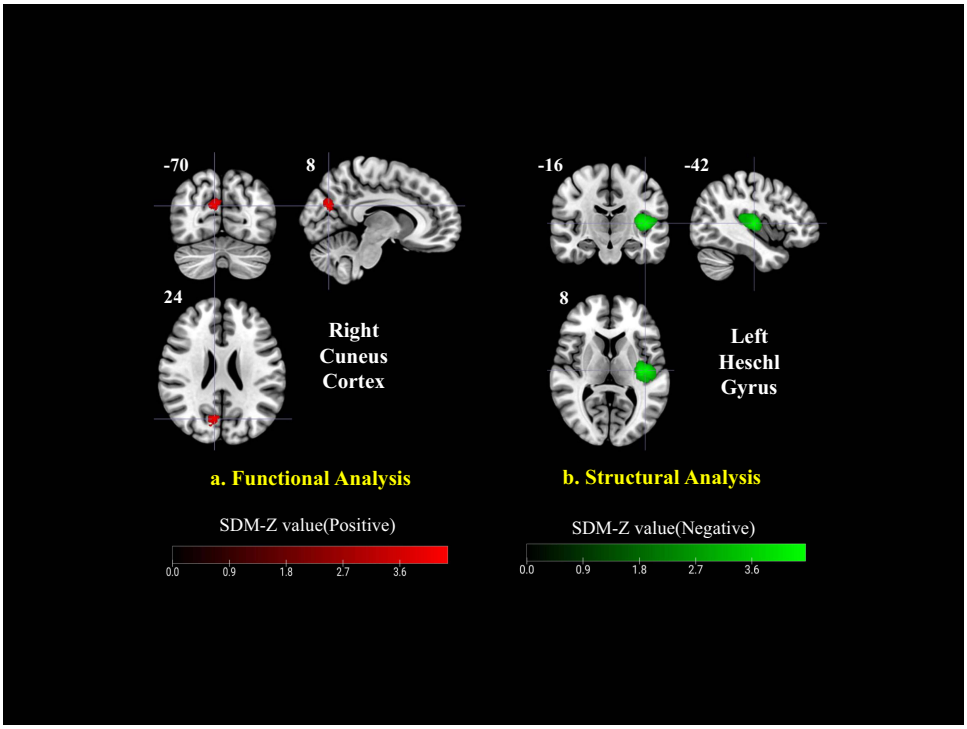

Figure 2 Functional and structural alterations in PHN vs HC. (**a**) Functional analysis revealed increased activation in the right cuneus cortex (red). (**b**) Structural analysis showed decreased gray matter volume in the left Heschl's gyrus (green). Color bars represent positive (red) and negative (green) SDM-Z values.

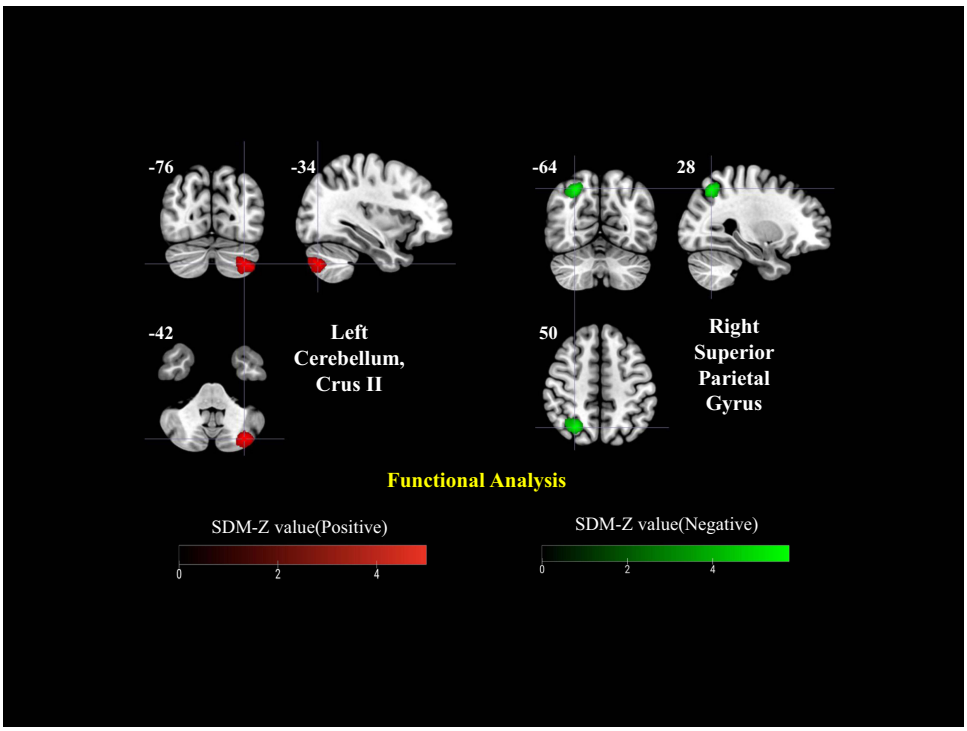

Figure 3 Functional alterations in PHN vs herpes zoster (HZ) patients. Increased activation was observed in the left cerebellum (Crus II), while decreased activity was found in the right superior parietal gyrus. Color bars represent positive (red) and negative (green) SDM-Z values.

https://doi.org/10.2147/JPR.S600570

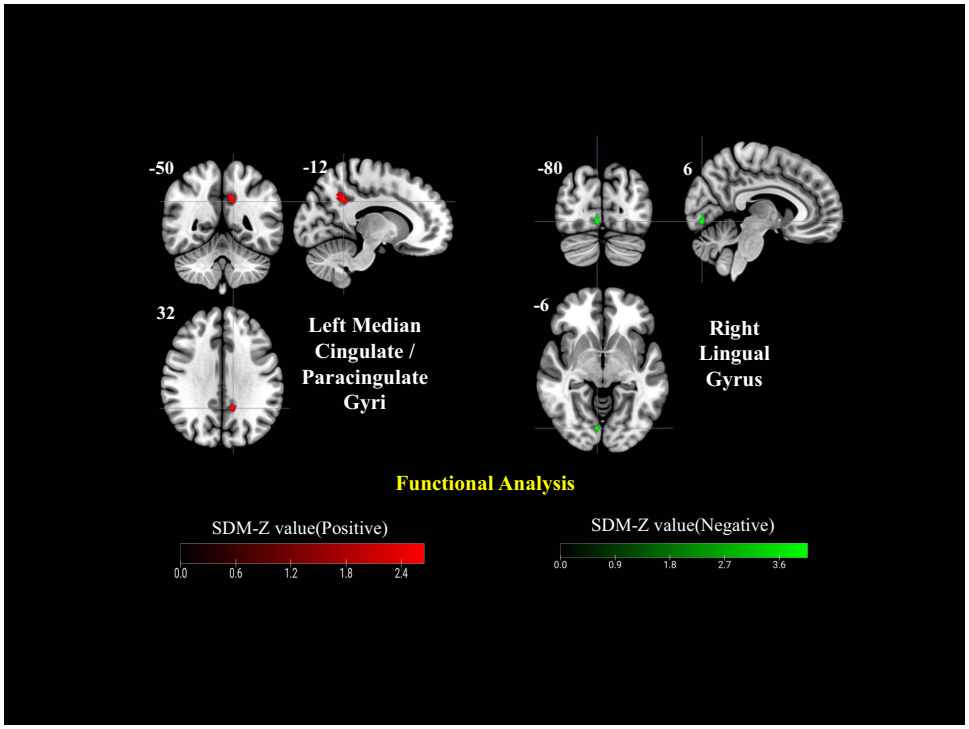

Figure 4 Longitudinal functional alterations in PHN (pre- and post-treatment comparison). Increased activity was detected in the left median cingulate/paracingulate gyri and decreased activity in the right lingual gyrus. Color bars represent positive (red) and negative (green) SDM-*Z* values.

Structural Alterations

Compared with HCs, PHN patients demonstrated GMV reductions predominantly in the left Heschl's gyrus, right precentral gyrus, left postcentral gyrus, and left median cingulate/paracingulate cortex, while no regions showed consistent GMV increases (Figure 2b).

Jack-Knife Sensitivity Analysis

The robustness of the meta-analytic results was assessed using a whole-brain jack-knife sensitivity analysis, in which the meta-analysis was iteratively repeated while excluding one dataset at a time. Regions that remained significant in most iterations were considered robust.

The results indicated that most main clusters of functional and structural alterations remained significant in most leave-one-out iterations, supporting the robustness of the principal findings. Specifically, in the PHN vs HC comparison, key functional regions such as the right cuneus cortex, left putamen, and right anterior thalamic projections remained significant in more than 70% of iterations (Table 2). Similarly, the left Heschl's gyrus and precentral/postcentral gyri in the structural analysis were retained in at least half of the iterations (3/6). Additional clusters identified in the supplementary jack-knife analyses are reported in Supplementary Tables 6–10.

In the PHN vs HZ comparison, the left cerebellum (Crus II) and right superior parietal gyrus (BA 7) remained significant in all six iterations (6/6), demonstrating excellent reproducibility across studies. The right cerebellum (Crus II) also showed consistent significance in most iterations (4/6), supporting stable cerebellar alterations between the two groups (Table 2 and Supplementary Tables 11–13).

In contrast, findings from the PHN pre- and post-treatment analysis showed limited reproducibility, with only a few regions, specifically the left median cingulate/paracingulate gyri and right lingual gyrus (BA 17), surviving in isolated iterations, suggesting greater heterogeneity in treatment-related effects (Table 2 and Supplementary Tables 14, 15).

https://doi.org/10.2147/JPR.S600570

Analysis of Heterogeneity and Publication Bias

We assessed between-study heterogeneity and potential publication bias across all significant clusters in the PHN vs HC, PHN vs HZ, and PHN pre- and post-treatment comparisons, as detailed in Supplementary Table 16 and Supplementary Figures 5–15.

For the PHN vs HC contrast (including both functional and structural imaging data), values of τ^2 and I^2 were generally low across significant clusters (I^2 ranging from 2.70% to 38.67%), indicating low-to-moderate between-study heterogeneity. Corresponding Q^2 values were non-significant in most clusters. Egger's test showed no significant evidence of small-study effects or publication bias (all $P > 0.05$), and excess significance tests were likewise non-significant.

In the PHN vs HZ functional contrast, heterogeneity indices remained low (I^2 ranging from 0.66% to 5.82%), and Egger's test did not indicate publication bias (all $P > 0.05$). However, due to the relatively small number of included datasets ($n = 6$), the statistical power of bias detection may be insufficient, and findings should be interpreted with caution.

Similarly, for the PHN pre- and post-treatment functional contrast, the number of studies did not meet the threshold for valid publication bias testing. Therefore, no funnel plot or Egger's test was performed for these contrasts.

Meta-Regression Analyses

Voxel-wise meta-regressions were performed to evaluate the effects of sex, age, education, pain duration, and VAS pain intensity on functional and structural alterations. Several significant moderator-dependent clusters were identified; however, none of these clusters overlapped with the main meta-analytic findings. This suggests that the core PHN-related abnormalities identified in the main meta-analysis were not primarily explained by the available demographic or clinical moderators. Detailed meta-regression statistics are provided in Supplementary Table 17.

Discussion

PHN as a Disorder of Large-Scale Brain Network Reorganization

To the best of our knowledge, this is the first whole-brain multimodal neuroimaging meta-analysis integrating resting-state spontaneous functional activity and structural gray matter alterations to characterize the central mechanisms of PHN. By synthesizing evidence across comparisons between PHN and healthy controls, PHN and herpes zoster patients, and longitudinal pre–post treatment data, our findings move beyond isolated regional abnormalities and instead support a systems-level model of PHN pathophysiology. This systems-level perspective is consistent with contemporary clinical frameworks that conceptualize PHN as a heterogeneous neuropathic pain condition involving interacting peripheral and central mechanisms, including central sensitization, impaired inhibitory modulation, and affective–cognitive dysfunctions.[44]

Collectively, the observed alterations converge on three interacting functional systems: (i) cross-modal sensory processing networks, (ii) affective–cognitive regulatory networks, and (iii) cortico–basal ganglia circuits involved in adaptive and maladaptive behavioral control. This framework provides a unifying explanation for how persistent nociceptive input following peripheral nerve injury may drive central sensitization, emotional distress, and pain chronicization in PHN.

Cross-Modal Sensory Processing Reorganization in PHN

A prominent finding of the present meta-analysis is the involvement of visual, auditory, and parietal association cortices, including the cuneus, fusiform gyrus, lingual gyrus, Heschl's gyrus, and superior parietal gyrus. Rather than indicating independent dysfunctions within individual sensory modalities, these alterations may suggest a broader reorganization of cross-modal sensory processing systems in PHN.

Chronic pain has increasingly been conceptualized as a condition characterized by altered sensory specificity and distributed perceptual processing, in which persistent nociceptive input may disrupt modality-specific boundaries and promote aberrant multisensory integration.[45] Within this framework, the involvement of occipital and visual association

cortices should be interpreted cautiously. Increased spontaneous activity in occipital regions does not necessarily indicate primary visual dysfunction in PHN, but may reflect altered visual–attentional engagement, pain-related hypervigilance, or broader cross-modal sensory integration under persistent nociceptive input.

This interpretation is also supported by neuroimaging findings from other chronic pain conditions. For example, visual-related regions such as the cuneus, lingual gyrus, fusiform gyrus, and occipital cortex have been reported in migraine[46] and chronic low back pain,[47] and occipital lobe abnormalities have also been described in HZ/PHN-related neuroimaging studies.[16] These observations suggest that visual cortical alterations may not be specific to PHN, but may represent a broader feature of chronic pain-related brain reorganization. Nevertheless, the precise role of visual association cortices in PHN remains unclear, and the present findings should therefore be regarded as hypothesis-generating rather than definitive.

Similarly, decreased activity in parietal areas may be associated with altered top–down allocation of attentional resources toward external sensory space. Structural alterations in auditory association cortex may further suggest that long-standing pain is associated with altered auditory–somatosensory integration, potentially contributing to sensory processing changes beyond the primary pain modality.

Affective–Cognitive Network Maladaptation and Emotional Burden in PHN

Beyond sensory processing, the present findings highlight substantial involvement of brain regions implicated in affective and cognitive regulation, particularly the medial cingulate/paracingulate cortex and bilateral cerebellar Crus II. These regions form core components of the medial pain pathway and salience-related networks that encode the affective and motivational dimensions of pain.

Importantly, contemporary models distinguish pain perception from pain-related suffering, proposing that suffering is mediated by distributed limbic and cingulate circuits rather than sensory-discriminative pathways alone.[48] Structural and functional abnormalities within the medial cingulate cortex observed in PHN therefore provide a neurobiological substrate for the emotional distress, rumination, and cognitive burden frequently reported in these patients.

Structural reductions in the cingulate cortex likely reflect long-term maladaptive plasticity induced by sustained emotional distress and pain-related rumination. In contrast, increased functional engagement of this region following treatment may represent compensatory reactivation of top–down regulatory mechanisms that modulate pain-related affect.

Beyond its classical role in motor coordination, the cerebellum—particularly Crus II—has been increasingly recognized as an integral component of cognitive–affective control networks involved in emotional regulation and internal monitoring of pain-related signals. Recent circuit-based models of chronic pain further emphasize that affective suffering and pain persistence are encoded across distributed cortico–limbic and cortico–basal ganglia circuits, and that effective treatment requires modulation of these circuits rather than suppression of nociceptive input alone.[49] Within this framework, heightened engagement of cerebellar Crus II in PHN may reflect maladaptive involvement of cognitive–affective control circuits that sustain pain-related emotional load.

Clinically, dysfunction within affective–cognitive networks provide a neural substrate for the high prevalence of anxiety, depression, and cognitive burden observed in PHN patients. These findings underscore the importance of addressing emotional and cognitive factors in PHN management and suggest that regions such as the cingulate cortex and cerebellum may serve as promising targets for neuromodulatory interventions, including non-invasive brain stimulation or integrative therapies aimed at alleviating both pain intensity and emotional suffering.

Cortico–Basal Ganglia Circuit Remodeling and Maladaptive Compensation

Another key contribution of this meta-analysis is the identification of altered activity within the lenticular nucleus and its associated cortical networks, pointing to maladaptive remodeling of cortico–basal ganglia circuits in PHN. These circuits play a central role in integrating sensory input with motivational, emotional, and motor planning processes, thereby shaping adaptive behavioral responses.

Hyperactivation of the putamen may reflect compensatory engagement aimed at maintaining behavioral readiness under persistent nociceptive stress. However, prolonged activation of this circuit may paradoxically reinforce pain-related

salience and maladaptive habits, contributing to pain persistence and reduced behavioral flexibility. This interpretation aligns with contemporary models that conceptualize chronic pain as a disorder of learning and prediction, in which maladaptive reinforcement mechanisms perpetuate pain experience even after peripheral pathology stabilizes.[50]

From a translational perspective, cortico–basal ganglia alterations may underlie impaired pain coping strategies and variable treatment responsiveness in PHN. Targeting this circuit through behavioral interventions, neuromodulation, or integrative therapeutic approaches may help disrupt maladaptive pain-related habits and facilitate functional recovery.

Integrated Clinical Implications and Future Directions

Taken together, the present findings support a reconceptualization of PHN as a disorder of large-scale brain network reorganization encompassing cross-modal sensory processing, affective–cognitive regulation, and cortico-basal ganglia

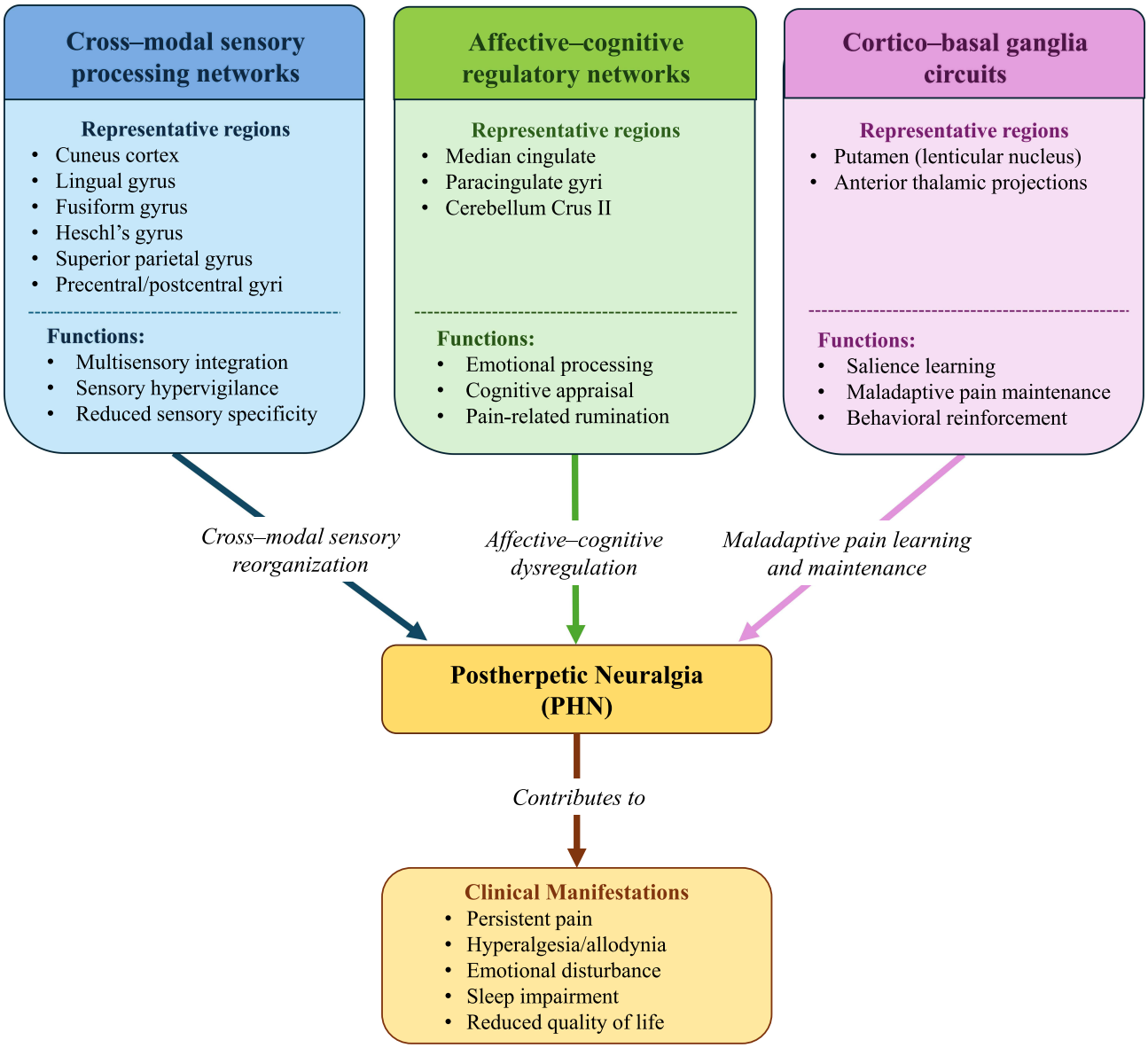

Figure 5 Schematic summary of large-scale brain network reorganization in postherpetic neuralgia. This figure summarizes the principal brain systems implicated in PHN based on the present voxel-wise meta-analysis, including cross-modal sensory processing networks, affective–cognitive regulatory networks, and cortico–basal ganglia circuits. These systems may interact to contribute to persistent pain, sensory hypervigilance, emotional disturbance, sleep impairment, and reduced quality of life. The figure is intended as a conceptual framework rather than a direct anatomical connectivity map. These network-level alterations may represent candidate neuroimaging biomarkers and potential therapeutic targets for future mechanism-guided interventions.

circuitry. Importantly, these network-level abnormalities may have potential clinical and translational implications. Rather than being viewed only as descriptive neuroimaging findings, the identified network-level alterations may provide candidate neuroimaging biomarkers for characterizing PHN-related disease state and pain chronicization, as well as preliminary treatment-related neuroimaging features reflecting treatment-related neuroplasticity. This interpretation is consistent with current neuroimaging-based pain biomarker frameworks, which emphasize diagnostic, prognostic, predictive, and treatment-response applications while requiring further validation before clinical use.[51,52] In this context, neuroimaging biomarkers may help characterize the central nervous system involvement of PHN beyond pain intensity alone, and may provide objective features for future mechanism-based patient stratification, prognosis prediction, and treatment-response monitoring.

These findings may also inform future therapeutic target selection. If PHN-related symptoms arise from interactions among pain processing, emotional regulation, cognitive control, and multisensory integration networks, clinical interventions should not focus exclusively on classical pain-related regions. Instead, network-modulating strategies may target affective–cognitive and multisensory systems to improve pain-related emotional distress, hypervigilance, and maladaptive sensory processing. For example, cingulate/paracingulate-related regulatory circuits may provide a potential framework for future neuromodulation approaches, such as repetitive transcranial magnetic stimulation (rTMS), transcranial direct-current stimulation (tDCS), or other non-invasive brain stimulation techniques; sensory association networks may be relevant to multisensory training or sensory reweighting strategies; and affective–cognitive circuits may be addressed through cognitive-behavioral strategies or integrative pain management.[53–55] Therefore, the present findings provide a preliminary neuroimaging framework for developing mechanism-guided interventions that go beyond peripheral analgesia and target maladaptive central network reorganization in PHN.

However, these clinical implications remain exploratory. The identified brain network alterations should be regarded as candidate biomarkers and potential therapeutic targets, rather than established clinical tools at this stage. Future longitudinal and interventional neuroimaging studies are needed to determine whether these network-level alterations can predict PHN development, symptom burden, or treatment response, and whether direct or indirect modulation of these networks can improve pain, emotional symptoms, and quality of life in PHN patients. To provide a more intuitive summary of the proposed network-level framework, we developed a schematic illustration of large-scale brain network reorganization in PHN (Figure 5).

Limitations

Several limitations of this meta-analysis should be considered. First, although we adopted the SDM-PSI framework and performed TFCE corrections to minimize false positives, the number of available neuroimaging studies on PHN remains relatively small, particularly for VBM and longitudinal designs. This limited sample size may reduce statistical power and constrain the detection of smaller or more heterogeneous effects. Second, heterogeneity across studies—including differences in MRI scanners, acquisition parameters, preprocessing pipelines, statistical thresholds, and pain duration—may contribute to variability in reported findings, despite our efforts to harmonize coordinates and apply strict inclusion criteria.

Third, heterogeneity across imaging modalities should be considered when interpreting the pooled findings. The resting-state indices included in this meta-analysis capture different aspects of spontaneous brain activity: ALFF and fALFF primarily reflect the amplitude of low-frequency fluctuations, whereas ReHo reflects local synchronization of neural activity. In contrast, VBM assesses structural gray matter volume rather than functional activity. Therefore, convergent findings across these modalities should be interpreted as complementary evidence of broad central involvement in PHN rather than as direct measures of the same biological process. Although SDM-PSI allows coordinate-based synthesis across studies, methodological differences in imaging metrics, preprocessing pipelines, statistical thresholds, and sample characteristics may contribute to heterogeneity and influence the interpretation of pooled results. Due to the limited number of available studies within each modality, more refined modality-specific subgroup analyses were not feasible. Future studies with larger datasets and harmonized acquisition and analysis protocols are needed to clarify modality-specific and cross-modal neuroimaging signatures of PHN.

Fourth, although meta-regression analyses were performed to explore the potential influence of demographic and clinical variables, the interpretation of these findings is limited by the small number of available datasets and inconsistent reporting of clinical measures across studies. The lack of spatial overlap between moderator-related clusters and the main meta-analytic findings suggests that the core PHN-related network abnormalities may not be primarily driven by the available demographic or clinical variables, such as age, pain duration, or VAS pain intensity. Alternatively, this negative finding may reflect the limited sensitivity of currently available clinical measures to capture the complexity of PHN-related brain network alterations. Future studies combining neuroimaging with multidimensional clinical, sensory, and psychological assessments are needed to clarify these relationships.

Fifth, the cross-sectional design of most included studies restricts causal interpretations regarding the temporal progression of PHN-related brain alterations. While the available longitudinal studies provided preliminary evidence for treatment-related modulation, the sample size remains insufficient to draw definitive conclusions.

Finally, coordinate-based meta-analysis inherently relies on reported peak coordinates rather than full statistical maps, which may overlook spatially distributed or subthreshold effects. Future research incorporating image-based meta-analysis, harmonized acquisition protocols, larger multicenter cohorts, and longitudinal designs will be essential for clarifying the dynamic neural mechanisms of PHN and improving translational applicability.

Conclusion

In conclusion, this multimodal voxel-wise coordinate-based meta-analysis demonstrates that PHN is characterized by convergent structural and spontaneous functional alterations across three large-scale brain network systems, namely cross-modal sensory processing systems, affective–cognitive regulatory networks, and cortico–basal ganglia circuits. These findings support PHN as a disorder of maladaptive central network reorganization rather than a collection of isolated regional abnormalities. Importantly, these network-level alterations may provide candidate neuroimaging biomarkers for characterizing PHN-related disease state and pain chronicization, as well as preliminary treatment-related neuroimaging features reflecting neuroplasticity. They may also provide potential therapeutic targets for future mechanism-guided and network-modulating interventions, including neuromodulation strategies. Further longitudinal and interventional neuroimaging studies are needed to validate their clinical utility as biomarkers or therapeutic targets and to clarify the causal mechanisms underlying PHN-related brain network plasticity.

Funding

This work was supported by the Beijing Traditional Chinese Medicine Science and Technology Development Fund (BJZZYB-2023-11) and the National Natural Science Foundation of China (Grant No. 82374555).

Disclosure

The authors report no conflicts of interest in this work.

References

1. Johnson RW, Rice AS. Clinical practice. Postherpetic neuralgia. *N Engl J Med*. 2014;371(16):1526–1533. doi:10.1056/NEJMcp1403062
2. Finnerup NB, Kuner R, Jensen TS. Neuropathic Pain: from Mechanisms to Treatment. *Physiol Rev*. 2021;101(1):259–301. doi:10.1152/physrev.00045.2019
3. Liu Q, Han J, Zhang X. Peripheral and central pathogenesis of postherpetic neuralgia. *Skin Res Technol*. 2024;30(8):e13867. doi:10.1111/srt.13867
4. May A. Chronic pain may change the structure of the brain. *Pain*. 2008;137(1):7–15. doi:10.1016/j.pain.2008.02.034
5. Li Y, Jin J, Kang X, Feng Z. Identifying and evaluating biological markers of postherpetic neuralgia: a comprehensive review. *Pain Ther*. 2024;13(5):1095–1117. doi:10.1007/s40122-024-00640-3
6. Tang Y, Wang M, Zheng T, et al. Structural and functional brain abnormalities in postherpetic neuralgia: a systematic review of neuroimaging studies. *Brain Res*. 2021;1752:147219. doi:10.1016/j.brainres.2020.147219
7. Müller VI, Cieslik EC, Laird AR, et al. Ten simple rules for neuroimaging meta-analysis. *Neurosci Biobehav Rev*. 2018;84:151–161. doi:10.1016/j.neubiorev.2017.11.012
8. Radua J, Mataix-Cols D. Meta-analytic methods for neuroimaging data explained. *Biol Mood Anxiety Disord*. 2012;2:6. doi:10.1186/2045-5380-2-6
9. WanYu C. *Postherpetic Neuralgia in Chest and Back Patients with Emotion Disorders: A Resting State Low Frequency Amplitude Study* [Master's thesis]. Chinese Medical Sciences University; 2019:1–33. (in Chinese). doi:10.27652/d.cnki.gzyku.2019.001021.
10. Yi Z. *Multimodal MRI-Based Study on Patients with Postherpetic Neuralgia* [PhD thesis]. Shanghai Jiao Tong University; 2016:1–88. (in Chinese). doi:10.27307/d.cnki.gsjtu.2016.003364.

11. Rujiao Y. *Brain Resting State-Functional Magnetic Resonance Study in Postherpetic Neuralgia* [Master's thesis]. Kunming Medical University; 2017:1–62. (in Chinese).
12. Xiang L, Fuyong C, Wei T, et al. Functional magnetic resonance imaging study on changes in basic brain activity in patients with postherpetic neuralgia. *Prog Biochem Biophys*. 2015;42(10):947–954. (in Chinese). doi:10.16476/j.pibb.2015.0095
13. Chengcheng J. *The Research of Postherpetic Neuralgia Patients with Resting State Functional MRI and Voxel Based Morphometry* [Master's thesis]. Suzhou University; 2017:1–49. (in Chinese).
14. Lala B, Wei Y, Miao Z, Guobiao H. Magnetic resonance imaging study of brain function and structure changes in patients with post-herpetic neuralgia. *Imaging Sci Photochem*. 2022;40(2):286–290. (in Chinese).
15. Song C. *Multimodal MRI Study on the Herpes Zoster Pain and Postherpetic Neuralgia* [PhD thesis]. Shanghai Jiao Tong University; 2017:3–95. (in Chinese). doi:10.27307/d.cnki.gsjtu.2017.000849.
16. Huang J, Li Y, Xie H, et al. Abnormal intrinsic brain activity and neuroimaging-based fMRI classification in patients with herpes zoster and postherpetic neuralgia. *Front Neurol*. 2020;11:532110. doi:10.3389/fneur.2020.532110
17. Cao S, Song G, Zhang Y, et al. Abnormal local brain activity beyond the pain matrix in postherpetic neuralgia patients: a resting-state functional MRI study. *Pain Physician*. 2017;20(2):E303–E314.
18. Gu L, Hong S, Jiang J, et al. Bidirectional alterations in ALFF across slow-5 and slow-4 frequencies in the brains of postherpetic neuralgia patients. *J Pain Res*. 2018;12:39–47. doi:10.2147/JPR.S179077
19. Dai H, Jiang C, Wu G, et al. A combined DTI and resting state functional MRI study in patients with postherpetic neuralgia. *Jpn J Radiol*. 2020;38(5):440–450. doi:10.1007/s11604-020-00926-4
20. Cao S, Li Y, Deng W, et al. Local brain activity differences between herpes zoster and postherpetic neuralgia patients: a resting-state functional MRI study. *Pain Physician*. 2017;20(5):E687–E699.
21. Wang S, Lu Y, Zhao W, et al. Observation of morphological changes of brain gray matter volume in patients with postherpetic neuralgia using VBM-DARTEL method. *J Pract Radiol*. 2017:1337–1340.
22. Tang Y, Ren C, Wang M, et al. Altered gray matter volume and functional connectivity in patients with herpes zoster and postherpetic neuralgia. *Brain Res*. 2021;1769:147608. doi:10.1016/j.brainres.2021.147608
23. Liu J, Gu L, Huang Q, et al. Altered gray matter volume in patients with herpes zoster and postherpetic neuralgia. *J Pain Res*. 2019;12:605–616. doi:10.2147/JPR.S183561
24. Niu L, Hu Y, Yuan CD, Wu XY, Zheng LL, Zhang Y. Cerebral structural alterations in the patients undergoing postherpetic neuralgia: a VBM–MRI study. *iBrain*. 2022;8(2):119–126. doi:10.1002/ibra.12027
25. Haowen L. *The Study of Cerebral Function in Postherpetic Neuralgia Pain by Rest State fMRI* [Master's thesis]. Guangdong Medical College; 2013:6–47. (in Chinese).
26. Haowen L, Lizu X, Yunhai Q, Qiang LX, Dongling LHX, Deren Z. The comparative study of cerebral function in different phases of herpes zoster by ReHO fMRI. *Chin J Pain Med*. 2014;20(10):717–721. (in Chinese).
27. Bu C, Ren H, Lv Q, et al. Alteration of static and dynamic intrinsic brain activity induced by short-term spinal cord stimulation in postherpetic neuralgia patients. *Front Neurosci*. 2023;17:1254514. doi:10.3389/fnins.2023.1254514
28. Zhang Y, Cao S, Yuan J, Song G, Yu T, Liang X. Functional and structural changes in postherpetic neuralgia brain before and six months after pain relieving. *J Pain Res*. 2020;13:909–918. doi:10.2147/JPR.S246745
29. Fan X, Ren H, Bu C, et al. Alterations in local activity and functional connectivity in patients with postherpetic neuralgia after short-term spinal cord stimulation. *Front Mol Neurosci*. 2022;15:938280. doi:10.3389/fnmol.2022.938280
30. Albajes-Eizagirre A, Radua J. What do results from coordinate-based meta-analyses tell us? *Neuroimage*. 2018;176:550–553. doi:10.1016/j.neuroimage.2018.04.065
31. Albajes-Eizagirre A, Solanes A, Vieta E, Radua J. Voxel-based meta-analysis via permutation of subject images (PSI): theory and implementation for SDM. *Neuroimage*. 2019;186:174–184. doi:10.1016/j.neuroimage.2018.10.077
32. Page MJ, McKenzie JE, Bossuyt PM, et al. The PRISMA 2020 statement: an updated guideline for reporting systematic reviews. *BMJ*. 2021;372:n71. doi:10.1136/bmj.n71
33. Iwabuchi SJ, Krishnadas R, Li C, Auer DP, Radua J, Palaniyappan L. Localized connectivity in depression: a meta-analysis of resting state functional imaging studies. *Neurosci Biobehav Rev*. 2015;51:77–86. doi:10.1016/j.neubiorev.2015.01.006
34. Pan P, Zhu L, Yu T, et al. Aberrant spontaneous low-frequency brain activity in amnestic mild cognitive impairment: a meta-analysis of resting-state fMRI studies. *Ageing Res Rev*. 2017;35:12–21. doi:10.1016/j.arr.2016.12.001
35. Radua J, Mataix-Cols D, Phillips ML, et al. A new meta-analytic method for neuroimaging studies that combines reported peak coordinates and statistical parametric maps. *Eur Psychiatry*. 2012;27(8):605–611. doi:10.1016/j.eurpsy.2011.04.001
36. Albajes-Eizagirre A, Solanes A, Radua J. Meta-analysis of non-statistically significant unreported effects. *Stat Methods Med Res*. 2019;28(12):3741–3754. doi:10.1177/0962280218811349
37. Pezzoli S, Emsell L, Yip SW, et al. Meta-analysis of regional white matter volume in bipolar disorder with replication in an independent sample using coordinates, T-maps, and individual MRI data. *Neurosci Biobehav Rev*. 2018;84:162–170. doi:10.1016/j.neubiorev.2017.11.005
38. Wang L, Liu R, Liao J, et al. Meta-analysis of structural and functional brain abnormalities in early-onset schizophrenia. *Front Psychiatry*. 2024;15:1465758. doi:10.3389/fpsyt.2024.1465758
39. Yu W, Tao B, Zhu F, et al. Shared cortical characteristics in major depressive disorder, anxiety disorder, and chronic pain: a structural MRI meta-analysis study. *Transl Psychiatry*. 2025;15(1):430. doi:10.1038/s41398-025-03424-1
40. Smith SM, Nichols TE. Threshold-free cluster enhancement: addressing problems of smoothing, threshold dependence and localisation in cluster inference. *Neuroimage*. 2009;44(1):83–98. doi:10.1016/j.neuroimage.2008.03.061
41. Higgins JP, Thompson SG, Deeks JJ, Altman DG. Measuring inconsistency in meta-analyses. *BMJ*. 2003;327(7414):557–560. doi:10.1136/bmj.327.7414.557
42. Egger M, Davey Smith G, Schneider M, Minder C. Bias in meta-analysis detected by a simple, graphical test. *BMJ*. 1997;315(7109):629–634. doi:10.1136/bmj.315.7109.629
43. Sterne JA, Sutton AJ, Ioannidis JP, et al. Recommendations for examining and interpreting funnel plot asymmetry in meta-analyses of randomised controlled trials. *BMJ*. 2011;343:d4002. doi:10.1136/bmj.d4002

44. Gilron I, Baron R, Jensen T. Neuropathic pain: principles of diagnosis and treatment. *Mayo Clin Proc*. 2015;90(4):532–545. doi:10.1016/j.mayocp.2015.01.018
45. Baliki MN, Apkarian AV. Nociception, pain, negative moods, and behavior selection. *Neuron*. 2015;87(3):474–491. doi:10.1016/j.neuron.2015.06.005
46. Wang M, Su J, Zhang J, et al. Visual cortex and cerebellum hyperactivation during negative emotion picture stimuli in migraine patients. *Sci Rep*. 2017;7:41919. doi:10.1038/srep41919
47. Chen X, Chen N, Lai P, et al. Multimodal abnormalities of brain function in chronic low back pain: a systematic review and meta-analysis of neuroimaging studies. *Front Neurosci*. 2025;19:1535288. doi:10.3389/fnins.2025.1535288
48. De Ridder D, Adhia D, Vanneste S. The anatomy of pain and suffering in the brain and its clinical implications. *Neurosci Biobehav Rev*. 2021;130:125–146. doi:10.1016/j.neubiorev.2021.08.013
49. Mercer Lindsay N, Chen C, Gilam G, Mackey S, Scherrer G. Brain circuits for pain and its treatment. *Sci Transl Med*. 2021;13(619):eabj7360. doi:10.1126/scitranslmed.abj7360
50. Apkarian VA, Hashmi JA, Baliki MN. Pain and the brain: specificity and plasticity of the brain in clinical chronic pain. *Pain*. 2011;152(3 Suppl):S49–S64. doi:10.1016/j.pain.2010.11.010
51. Mackey S, Greely HT, Martucci KT. Neuroimaging-based pain biomarkers: definitions, clinical and research applications, and evaluation frameworks to achieve personalized pain medicine. *Pain Rep*. 2019;4(4):e762. doi:10.1097/pr9.0000000000000762
52. Zhang LB, Chen YX, Li ZJ, et al. Advances and challenges in neuroimaging-based pain biomarkers. *Cell Rep Med*. 2024;5(10):101784. doi:10.1016/j.xcrm.2024.101784
53. Gao C, Zhu Q, Gao Z, Zhao J, Jia M, Li T. Can noninvasive brain stimulation improve pain and depressive symptoms in patients with neuropathic pain? A systematic review and meta-analysis. *J Pain Symptom Manage*. 2022;64(4):e203–e215. doi:10.1016/j.jpainsymman.2022.05.002
54. Kong Q, Li T, Reddy S, Hodges S, Kong J. Brain stimulation targets for chronic pain: insights from meta-analysis, functional connectivity and literature review. *Neurotherapeutics*. 2024;21(1):e00297. doi:10.1016/j.neurot.2023.10.007
55. Xiong HY, Zheng JJ, Wang XQ. Non-invasive brain stimulation for chronic pain: state of the art and future directions. *Front Mol Neurosci*. 2022;15:888716. doi:10.3389/fnmol.2022.888716